Natural Resources for Human Health
eISSN: 2583-1194

Original Research

Received 21 May 2026
Revised 30 June 2026
Accepted 23 July 2026

Natural Resources for Human Health 2026, Vol. 6 (10s): 475–494

KEYWORDS:
Electrospinning, Nanofibers, Polymers, MXene, MAX, Water Treatment.

Synergistic Integration of 2D MXenes into Electrospun Nanofibers: From Microstructural Tailoring to Advanced Environmental Remediation

Israa M. Rashid[1], Alaa Kareem Mohammed[2]*, Mustafa H. Al-Furaiji[3]

[1]Biochemical Engineering Department, Al-Khwarizmi College of Engineering, University of Baghdad, Baghdad 47024, Iraq; https://orcid.org/0000-0002-5209-6767
[2]Biochemical Engineering Department, Al-Khwarizmi College of Engineering, University of Baghdad, Baghdad 47024, Iraq; https://orcid.org/0000-0002-2765-9142
[3]Scientific Research Commission, Baghdad, Iraq; https://orcid.org/0000-0002-7373-9370
*Corresponding Author: dr.alaa@kecbu.uobaghdad.edu.iq, 009647718612291

ABSTRACT: Membrane technology has become an integral part of wastewater treatment and environmental remediation. Among various methods of fabrication, electrospinning has drawn significant attention due to its ability to produce highly porous membranes with interconnected pore structures, high specific surface area and controllable fibre diameter. At the same time, MXenes, a newly emerged family of two-dimensional (2D) transition metal carbides, nitrides, and carbonitrides have revolutionised the paradigms of the materials science due to their hydrophilic surface chemistry, metallic electrical conductivity and excellent chemical tunability. In this review, we present a comprehensive discussion on the synergistic integration of electrospun nanofiber membranes with MXenes in water purification. The fundamentals of electrospinning, the methods to embed MXenes into polymer matrices and the morphological modifications are thoroughly discussed. We comprehensively review the performance of these composite membranes for oil-water separation, heavy metals removal and desalination, elucidating the underlying principles and addressing the current scaling-up and stability challenges.

1. INTRODUCTION

Access to clean water is still one of the biggest problems of the 21st century (Damptey et al. 2022; Waisi et al., 2026). According to the United Nations World Water Development Report (2023) ('UNESCO World Water Assessment Programme (WWAP), Water for People, Water for Life: The United Nations World Water Development Report' 2003), rapid industrialisation, population growth, and urbanisation have worsened water pollution. More than 80% of the world's wastewater is discharged into ecosystems untreated. Heavy metals (like $Pb^{2+}, Cd^{2+},$ and Cr^{6+}), organic dyes (like methylene blue and Congo red), pharmaceuticals, and new micropollutants are all very dangerous to aquatic life, human health, and food security (Date and Jaspal, 2024; Kadhom et al., 2020). Traditional treatment methods, such as ion exchange, activated carbon adsorption, chemical precipitation, and biological processes, have significant drawbacks: elevated operational costs, limited pollutant removal, production of hazardous sludge, and susceptibility to fouling (Crini et al., 2019; Rajasulochana and Preethy, 2016).

Nanotechnology provides revolutionary solutions via materials characterised by elevated surface-to-volume ratios and customised functionalities (Mekuye and Abera, 2023). MXenes, a family of two-dimensional (2D) transition-metal carbides,

nitrides, or carbonitrides, have attracted significant attention since their discovery by Naguib et al. at Drexel University in 2011 (Crini et al., 2019).

MXenes are a family of two-dimensional transition metal carbides, nitrides and carbonitrides with the general formula $M_{n+1}X_nT_x$, obtained through the selective etching of the A-layer from MAX phases (Kumar and Taunk, 2024). Their relevance to water-treatment membranes is not only due to their novelty but also because of the collection of features that directly reduce key membrane constraints (Seling et al., 2025; Sun et al., 2024a). Hydrophilic surface terminations, such as $-OH$ and $-O$, allow strong interactions with water and a reduction in pollutant adhesion (Imsong and Dhar Purkayastha, 2023). The increased surface area and the tunable interlayer spacing allow selective transport and ion sieving (Jain et al., 2026). Moreover, they possess chemically modifiable surfaces to further customise wettability and interfacial interactions, which are crucial to improve antifouling properties and separation efficiency (Zhang et al., 2023). Thus, MXenes are better classified as functional membrane modifiers and not as inert fillers especially in the case of electrospun nanocomposites for advanced water treatment applications.

Electrospinning transforms MXenes into practical, large-scale configurations by producing nanofibers with diameters ranging from 50 to $500\ nm$ (Wafaa Kh. Al-Musawy et al., 2026; Li et al., 2024; Pant et al., 2023a). This method uses high voltage on a polymer-MXene solution to shoot out a charged jet that hardens into a nonwoven mat (Khadem et al., 2025b; Raut et al., 2025; Wang et al., 2025, 2024; W. Wu et al., 2025a). Adding MXenes $(1-10\ wt\%)$ to polymers like PVDF, PAN, or chitosan makes nanocomposites that work together in a way that makes them stronger. (Gao et al., 2019a, 2019b; Jain et al., 2026; Qin et al., 2022; Wang et al., 2024):

- Enhanced tensile strength and flexibility.
- Improved antifouling via MXene's bactericidal effects (e.g., ROS generation).
- Hierarchical porosity for superior mass transfer.

Recent studies demonstrate adsorption capacities exceeding 500 mg/g for dyes and >200 mg/g for heavy metals, with regeneration efficiencies >90% over multiple cycles (Chen et al., 2024; Feng et al., 2021; Hou et al., 2023; Jun et al., 2020).

This review methodically assesses MXene-based electrospun nanocomposites for water treatment applications. It discusses ways to make things (e.g., in-situ etching and electrostatic complexation), ways to test them (e.g., SEM, XRD, XPS, and BET), how well they perform in batch and flow systems, and how they work (e.g., electrostatic attraction, π-π stacking, and photocatalysis). We look closely at important problems, like MXene oxidation, the scalability of electrospinning, and long-term stability. We also look at solutions, like hetero structuring with TiO_2 or $g-C_3N_4$. Future directions stress pilot-scale deployment, life-cycle assessments, and integration with membrane bioreactors for sustainable, real-world uses.

This work highlights the potential of MXene electrospun nanocomposites to transform decentralised water purification by addressing gaps in synthesis, application, and innovation, in accordance with UN Sustainable Development Goal 6 (Kamto, 2016). In Scheme 1, there is a brief graph about the content of this review article.

Scheme 1. Main content of this review.

Natural Resources for Human Health
eISSN: 2583-1194

2. ELECTROSPINNING FUNDAMENTALS AND SOLUTION PARAMETERS

One benefit of electrospinning technology is the ability to customise the structure, which can be tailored to individual requirements by adjusting electrospinning settings or the device's design. Electrospinning is an efficient and straightforward technique for synthesizing nanofibers (Jabur et al., 2017).The electrospinning apparatus primarily consists of a high voltage source, a spinneret, and a collector, as shown in **Figure 1** (Alfalluji, 2025). The polymer solution is propelled from a hypodermic through a needle by a pump. The potential difference between the needle and the drum causes the solution to form a filament at the needle's tip, which is subsequently attracted to the collector plate (the drum). The polymer solution traverses the electric field, generating a liquid jet aimed at the collector. The swift evaporation of the solvent in the polymer solution transforms this jet into a fibre. The procedural stages of the process include (K. Wu et al., 2025):

i. preparation of the solution.

ii. Electrostatic field application.

iii. Cone-jet formation.

iv. Jet acceleration and stretching.

v. Collection of fibers.

vi. Parameter optimization.

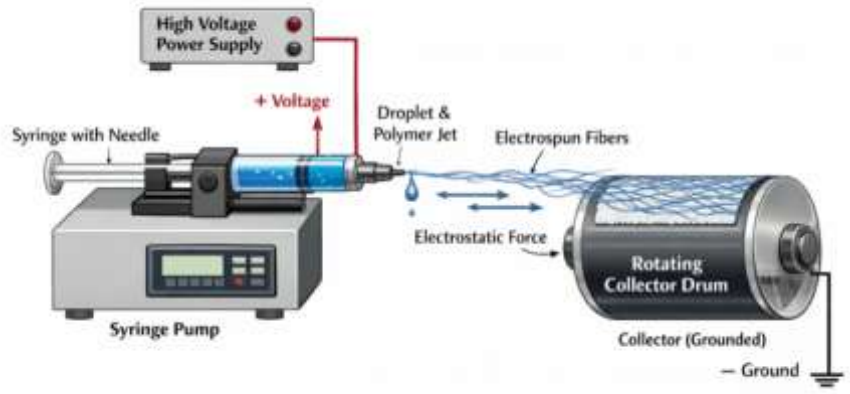

Figure 1: Schematic of an electrospinning apparatus. "AI assisted copy editing".

2.1 Electrospinning parameters

The electrospinning process is extremely sensitive to various parameters. These parameters are generally categorized into solution properties, processing conditions, and ambient parameters. Fine-tuning of these parameters is essential for the transition from "beading" (droplet formation) to high-quality, continuous nanofibers (Ahmadi Bonakdar and Rodrigue, 2024; Bonakdar and Rodrigue, 2024; D. Ji et al., 2024; Nadaf et al., 2022; Panditkar et al., 2025).

1. Solution Parameters

These are inherent to the chemical makeup of the mixture (like your PVA/MXene solution) (Ye et al., 2024).

- **Concentration & Viscosity:** These are the most critical factors. If the concentration is too low, surface tension dominates, leading to the jet breaking into droplets (**beading**). If it is too high, the solution becomes too viscous to flow through the needle (Carroll-Bassham and Brettmann, 2024; D. Ji et al., 2024).

- **Molecular Weight:** Higher molecular weight polymers provide the necessary chain entanglement to stabilize the jet (Cui et al., 2020; Gao et al., 2019b; Munshi et al., 2026).

- **Conductivity/Surface Charge:** Adding salts or conductive fillers (like **MXene**) to the jet's surface charge makes it more unstable and makes the fibres thinner (Cui et al., 2020).

- **Surface Tension:** High surface tension makes it hard to start the jet. To lessen this, surfactants are sometimes added (Yan et al., 2022).

2. Processing Parameters

- **Applied Voltage:** To form a Taylor Cone, you need a specific voltage. Higher voltage usually makes fibres thinner because it increases electrostatic repulsion. However, excessive voltage can cause multiple jets and fibres of different diameters (Panditkar et al., 2025).

- **Flow Rate:** This tells you how much solution is at the tip of the needle. If the flow rate is too high, the fibres won't have enough time to dry before reaching the collector, which can cause them to stick together or remain "wet" (Panditkar et al., 2025).

- **Distance from Tip to Collector:** • The distance from the tip to the collector must be adequate to facilitate the complete depletion of the solvent and the "whipping" stretching process (Cui et al., 2020; Liu et al., 2021; Qian et al., 2022; W. Wu et al., 2025a).

- **Needle Gauge (Diameter):** Smaller internal diameters can reduce clogging and produce finer fibers, though they require higher pump pressure (Ahmadi Bonakdar and Rodrigue, 2024; Yu and Tan, 2025).

3. Ambient Parameters

The environment surrounding the setup can significantly alter the final product.

- **Humidity:** High humidity can cause small pores to form on the fiber surface (due to "breath figures") or accelerate the polymer's precipitation (Mailley et al., 2021; D. Zhang et al., 2020).

- **Temperature:** Increasing the temperature usually decreases the solution's viscosity and increases the rate of solvent evaporation (Yang et al., 2017).

3. STRUCTURE, SYNTHESIS, AND PEELING OF MXENES

MXenes are a family of 2D transition-metal carbides, nitrides and carbonitrides from the periodic table, as shown in **Figure 2** (Pant et al., 2023b) obtained from MAX phases by selective removal of the A-layer (Abdul-Hussein et al., 2024; Pogorielov et al., 2021). Their general formula is $M_{(n+1)}X_nT_x$, where M is an early transition metal, X is carbon and/or nitrogen, and T_x is surface termination groups such as –OH,–O, and –F (Kadhom et al., 2022). The layered architecture together with chemically active surface terminations endow MXenes with a unique combination of hydrophilicity, high surface area, tunable interlayer spacing and strong interfacial reactivity, which is particularly relevant for membrane and nanocomposite applications (Pant et al., 2023b).

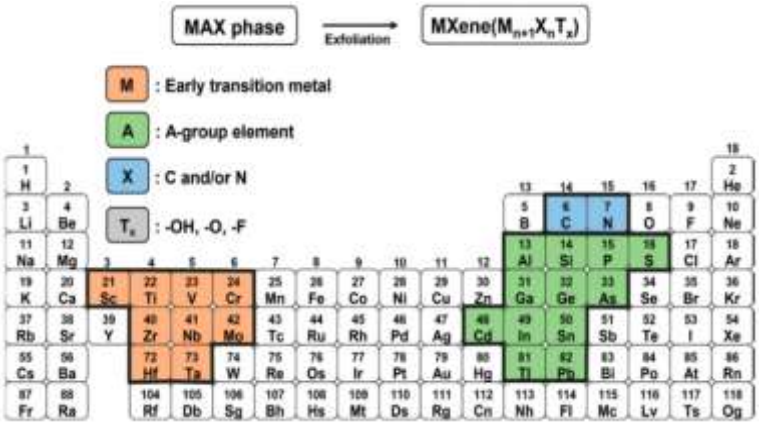

Figure 2: Periodic table showing the composition of the MAX phase and MXene (Pant et al., 2023b) licensed under CC BY 4.0.

The synthesis method is very important for the structure, surface chemistry and dispersion properties of MXenes in polymer matrices (Patial et al., 2025). Wet chemical etching (Jin et al., 2023) is the most established technique, whilst fluoride-salt-assisted etching (Zhu et al., 2023), hydrothermal treatment (Zhang et al., 2023), electrochemical etching (Liu et al., 2023) and molten-salt methods (Wang et al., 2023) have been developed to improve safety, surface control and scalability. Each route has trade-offs in etching efficiency, structural integrity, environmental impact and accessibility. Therefore, for the application of MXenes in electrospun membranes for water purification, the synthesis process needs to be carefully considered (Raut et al., 2025). Table 1 summarizes the commonly used methods for MXene synthesis, along with their advantages and disadvantages.

The synthesis routes dictate the structural quality, surface chemistry and dispersion characteristics of MXenes, all of which directly impact polymer compatibility, membrane formation and ultimate separation performance.

3.1 Wet chemical (HF etching)

The moist chemical process is the most widely researched method for producing MXene. For instance, the initial MXene, $Ti_3C_2T_x$, was extracted using 50% HF and Ti_3AlC_2 as the MAX phase (K. Ji et al., 2024). Subsequently, more MXenes, including $Hf_3C_2Tx, Ti_3CNTx,$ and Ti_2CTx, have been synthesised via the HF etching technique (Kiran et al., 2025). Consider HF etching aluminium atoms from Ti_3AlC_2 as a case study. The acquisition of single-layer or few-layer MXene materials entails two processes: an etching procedure followed by an exfoliation treatment, as illustrated in **Figure 3** (Antony Jose et al., 2025).

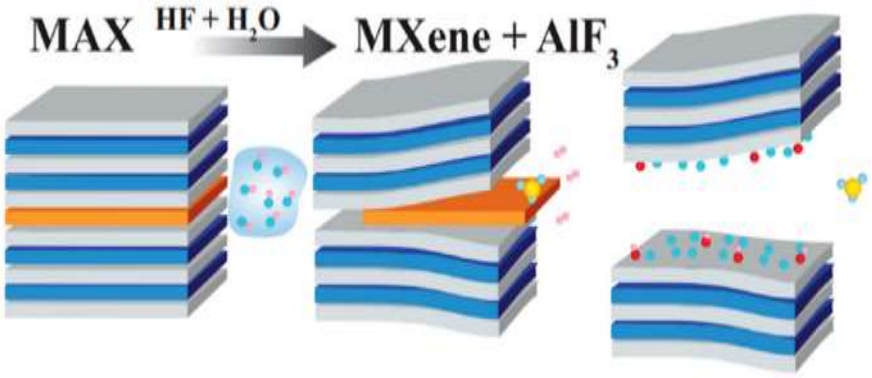

Figure 3: Schematic representation of the exfoliation process of MXenes from MAX phases, Reproduced from (Antony Jose et al., 2025), licensed under CC BY 4.0

3.2 Etching using strong acid and fluoride salt

Researchers offered enhanced strategies to circumvent the direct use of HF as an etching agent. An efficient technique involves a mixture of fluoride salt and HCl instead of HF. Consequently, the MAX phase will be etched in situ by the generation of HF when the MAX phase is submerged in a mixture of fluoride and HCl. Ghidiu et al. synthesised two-dimensional. Ti_3C_2 by etching Ti_3AlC_2 in a solution of LiF and HCl. Upon hydration, the hydrophilic substance expands in volume, can be moulded like clay, and can be dried to form a highly conductive solid or coatings that are many tens of micrometres thick (Kiran et al., 2025). **Figure 4** (Zhu et al., 2023) depicted a typical operation.

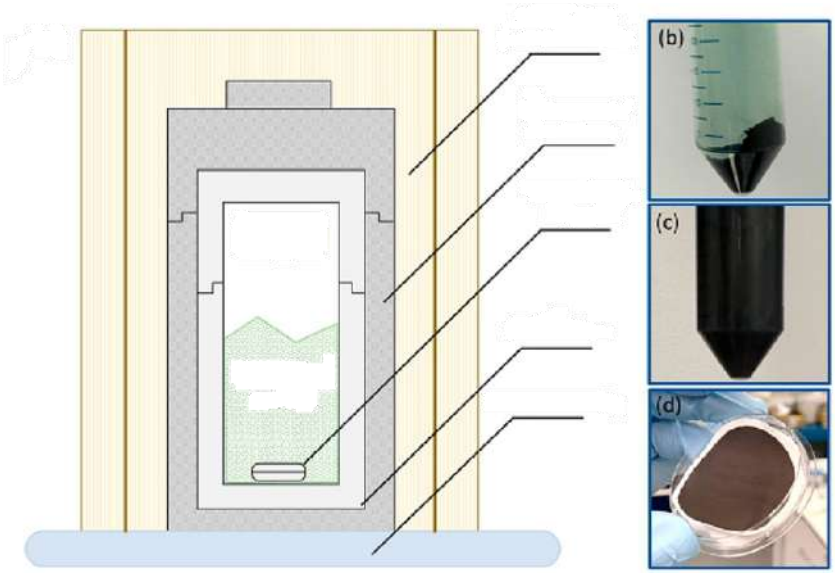

Figure 4: Improved fluoride salt and HCl etching process to prepared V_2C MXene, Reproduced from (Zhu et al., 2023), licensed under CC BY 4.0.

3.3 Hydrothermal

MXenes are synthesised via the hydrothermal reaction of MAX phases using alkali metal hydroxides (e.g., $NaOH, KOH$) under high temperature and pressure conditions. This approach is scalable and does not require hazardous HF, unlike the wet chemical procedure. Monolayer $Ti_3C_2(OH)_2$ was synthesised using KOH at $180\ °C$ for $24\ hours$ in an autoclave (Peng et al., 2018). Notwithstanding its scalable characteristics, the temporal and high temperature-pressure prerequisites limit its use for large-scale synthesis. **Figure 5** (Hada et al., 2022) illustrates the hydrothermal etching of Ti_3AlC_2 MAX to synthesize Ti_3AlC_2Tx MXene.

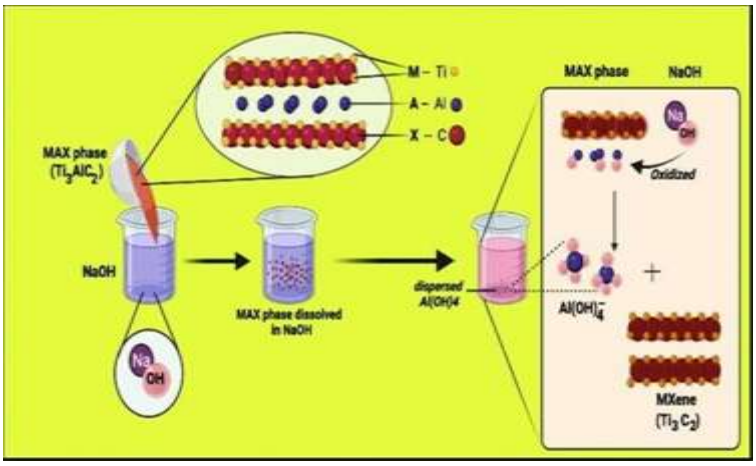

Figure 5: Schematic illustration of hydrothermal etching $Ti3AlC2$ MAX to synthesize Ti_3AlC_2 MXene, Reproduced from (Hada et al., 2022), licensed under CC BY 4.0.

3.4 Electrochemical

To etch using the electrochemical method, a cathode, an anode, and a direct current bias are required. Numerous studies have illustrated the use of electrolytes like $HCl, NaCl,$ and HF for the electrochemical etching of the MAX phase. Using such a route, Ti_2CTx, a fluorine-free MXene for the first time, was successfully synthesized (Yan et al., 2023). The electrochemical approach may excessively etch the MAX phase, potentially altering the structure of MXenes, despite its simplicity. Pang et al. synthesised Ti_2CTx using electrochemically etching of Ti_2AlC in an HCl solution. As seen in **Figure 6A** (Zhu et al., 2023), the etching method comprises two steps. The Al atom in Ti_2AlC was initially removed using an applied voltage due to the weaker

Natural Resources for Human Health
eISSN: 2583-1194

$Ti - Al$ bond relative to the $Ti - C$ bond. The comprehensive etching reaction on Ti_2AlC is delineated as follows (Zhu et al., 2023):

$$Ti_2AlC + yCl^- + (2x + z)H_2O \longrightarrow Ti_2C(OH)_{2x}Cl_yO_z + Al^{+3} + (x + z)H_2 + (y + 3)e^- \ldots\ldots\ldots (6)$$

As seen in **Figures 6B–D**, two bulk pieces Ti_3AlC_2 were employed as electrodes. The cathode served as the counter electrode in this configuration, resulting in etching exclusively on the anode's surface. In the context, TMA-OH fulfils two functions. Initially, it is a component of the electrolyte that contains NH_4Cl. Furthermore, $TMA - OH$ would dissociate into TMA^+ and OH^-.

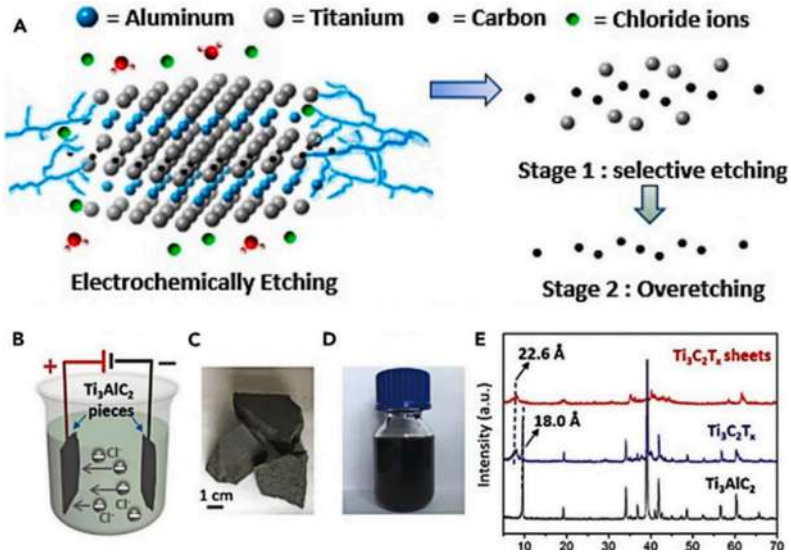

Figure 6: Electrochemical etching in aqueous solution, Reproduced from (Zhu et al., 2023)licensed under CC BY 4.0.

3.5 Molten salt etching

MXenes are extracted from unconventional MAX phases using the Lewis-acid-mediated molten-salt method. In 2019, Cl ended MXenes, namely. $Ti_3C_2Cl_2$ and Ti_3CCl_2, were separated using this approach (Khadem et al., 2025b). Furthermore, MXenes, both with and without surface termination groups, can be synthesised by the molten salt method, as documented by Kamysbayev et al. (Kamysbayev et al., 2020). So, by altering the surface chemistry, the molten salt method opens new uses for MXenes. **Figure 7** shows a diagram of the synthetic process (Liu et al., 2023).

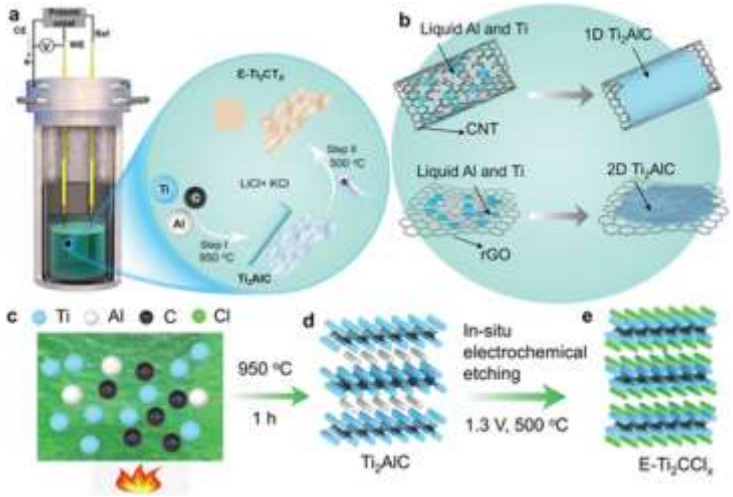

Figure 7: Schematic illustration of the fabrication process of Ti_2AlC and E-Ti_2CT_x. a) The schematics of the molten salt cell with the (Ti, Al, C) pellet, Reproduced from (Liu et al., 2023), licensed under CC BY 4.0.

4. INTEGRATION OF MXENES INTO POLYMERIC ELECTROSPUN MATRICES

Integration of MXenes into polymeric electrospun matrices is an effective strategy to obtain multifunctional nanofibrous membranes with improved mechanical integrity, surface functionality and separation performance (Abraham Swu and Dhar Purkayastha, 2025). MXenes are incorporated into electrospun systems either by post-electrospinning surface modification (decorating the nanofiber scaffold with MXene) (Zhu et al., 2026) or pre-electrospinning blending (dispersing MXene nanosheets in the polymer dope prior to fibre formation) (Buzgo et al., 2018). Both approaches have distinct advantages in terms of filler distribution, interfacial contact and control over membrane architecture.

The successful integration of MXene is highly dependent on the compatibility of MXene nanosheets with the host polymer and the dispersion quality achieved during processing (FitzPatrick and Gogotsi, 2025). The high aspect ratio, hydrophilic surface terminations and surface charge of MXenes promote interfacial interactions with polar polymers such as PAN, PVDF, PVA and chitosan, leading to improved rheological properties of the electrospinning solution and the formation of uniform nanofibers (Qin et al., 2022; Renkler et al., 2025; Wang et al., 2024). At optimum loading levels, MXenes are able to decrease the fibre width and improve the electrical conductivity and enhance the tensile strength by better load transfer and interfacial bonding (Said et al., 2025).

MXene integration needs careful optimisation, as excessive loading can lead to agglomeration of nanosheets, instability of the solution and irregular fibre shape (W. Wu et al., 2025a). These changes can alter pore shape, reduce effective flow and negatively affect membrane performance. The final microstructure and functional properties of the obtained composite membrane are jointly determined by the combination of polymer, solvent system, MXene concentration and electrospinning parameters (Santhamoorthy et al., 2025).

Two dominant fabrication methods are often cited. In the process of mix electrospinning, MXene nanosheets are directly dispersed in the polymer solution before the spinning, which can guarantee the uniform distribution in the fibre network (Li et al., 2024). On the other hand, the surface decoration techniques are mainly restricted to the outer surface of the fibre, which is beneficial for applications where enhanced surface accessibility, higher hydrophilicity and quicker interfacial interactions with the feed solution are required (Xue and Zhang, 2022). Altogether such approaches provide a flexible platform to tailor electrospun membranes for water treatment, sensing and a multitude of advanced filtration applications (Cui et al., 2020).

Membrane performance is determined by the fabrication method, MXene content, polymer chemistry, solvent selection and electrospinning parameters, all of which influence fibre morphology and separation efficiency. Table 2 summurize various MXene -polymer nanocomposites membrane for water treatment.

4.1 Blend Electrospinning (Composite Nano-architectures)

Blend electrospinning creates composite nanofibers with filler scattered throughout the membrane's bulk by immediately dispersing delaminated MXene nanosheets into the polymer dope solution before fibres are formed (Buzgo et al., 2018). This method is extensively utilised due to its operational simplicity, scalability, and compatibility with prevalent membrane-forming polymers including PAN, PVDF, PVA, chitosan, and PU. MXene enhances the electrical conductivity of the spinning solution and fortifies the electrostatic stretching of the jet, frequently resulting in diminished fibre diameter, more uniform morphology, and enhanced interfacial adhesion between the filler and polymer chains (Bachs-Herrera et al., 2021).

This technique works very effectively if the nanosheets are well dispersed and the MXene loading is appropriate (L. Zhou et al., 2025). MXene at moderate concentrations enhances mechanical reinforcement, hydrophilicity and surface functionality, but excessive loading can cause aggregation, bead formation and rheological instability, compromising ultimately fibre continuity and membrane porosity (Pan et al., 2026). Thus, tuning the filler content is critical to preserve the structural integrity of the electrospun network and to enhance the functional advantages of the MXene phase.

4.2 Surface Decoration and Modification

Another approach is surface decoration and coating, where MXene is mainly located on the outer surfaces of electrospun fibres or as a functional layer on existing mats. This method increases the surface accessibility of active MXene sites, which is especially desirable for adsorption, antifouling, catalytic degradation and oil/water separation, unlike bulk blending. Furthermore, limiting the MXene on the membrane surface can reduce the filler loss, promote the hydrophilicity more efficiently, and create a highly reactive separation interface without greatly altering the inner pore structure of the electrospun scaffold (Pan et al., 2026).

This method can be performed via dip coating (Dhamodharan et al., 2024), vacuum filtration (Imsong and Dhar Purkayastha, 2023), spray deposition (Abraham Swu and Dhar Purkayastha, 2025), layer-by-layer assembly (Zhu et al., 2023), or self-assembly (C. Zhang et al., 2020), depending on the required membrane architecture and application. Surface modification, though requiring additional processing steps, offers better control over the thickness of functional layers and interfacial chemistry compared to simple blending. It is thus often preferred when the required surface performance is more important than the bulk reinforcement (C. Zhang et al., 2020).

4.3 Fabrication Considerations

The optimum efficacy of MXene-polymer electrospun membranes is governed by a variety of processing parameters such as polymer type, MXene concentration, solvent composition, and electrospinning conditions (Dhamodharan et al., 2024; Riazi et al., 2021; W. Wu et al., 2025a; C. Zhang et al., 2020). The strong interactions between polar polymers and MXene surface terminations generally lead to better dispersion stability and favour optimal jet formation in the spinning process (Kumar et al., 2025). In the same way, the solvent polarity and evaporation rate influence the solution homogeneity, while the applied voltage, flow rate, tip-to-collector distance, humidity, and temperature determine the fibre diameter, bead formation, and architecture of the pores(Castellanos-Espinoza et al., 2025).

The selection between blending or surface decoration should be determined by the desired trade-off between mechanical reinforcement and surface function (Mannafi et al., 2025). Blended electrospinning is suitable for obtaining uniform filler dispersion and improving bulk structures (Buzgo et al., 2018), while surface decorating is beneficial for maximising interfacial interactions and the accessibility of active sites (Buzgo et al., 2018). The differentiation of water treatment membranes is of paramount importance, since separation efficiency, flow, fouling resistance and long-term stability are closely related to the position and distribution of MXene in the membrane structure.

4.4 Fabrication techniques of MXene-integrated membranes

MXene–polymer hybrid membranes are fabricated from MXene–polymer precursors using various synthesis strategies. Before discussing the fabrication of MXene–polymer hybrid membranes, it is essential to understand the fundamentals of MXene fabrication (Bisht et al., 2024; Khadem et al., 2025b; Pant et al., 2023a; Parajuli et al., 2022; Wang et al., 2024). This is because presynthesized MXenes are used during the architecture of MXene–polymer membranes.

4.4.1 Surface grafting or modifying MXenes

MXene sheets undergo chemical surface modification to add functional groups. These modified sheets are then integrated into polymer solutions through melting or mixing. The MXenes become physically entangled with or covalently linked to polymer chains during crosslinking, forming the final nanocomposite. S-MXene/S-ENR nanosheets are esterified with serine (using EDC/DMAP) and combined with amino-modified epoxidase natural rubber (ENR) to form a $3D$ network film at $100℃$ for three hours (Jain et al., 2026). This surface modification technique improves the compatibility between MXenes and various polymers, thereby enhancing the properties of the resulting hybrid materials.

4.4.2 Direct physical mixing

The most prevalent approach for creating MXene-reinforced polymer composites is the direct mixing of MXene with polymers. Linear thermoplastic polymers (such as TPU, PLA, and PP) are heated to a molten state and then thoroughly mixed with MXenes under constant stirring. For instance, MXene and TPU can be processed in an internal mixer at $160\ ℃$ and $400\ rpm$ for five minutes to create a uniform blend before compression. This method is also effective for creating complex reinforced composites, such as combining MXene nanosheets with short aramid fibers (SAF) in a polypropylene (PP) matrix (L. Zhou et al., 2025).

4.4.3 In situ polymerization

During this process, monomers (like pyrrole, aniline, or EDOT) are polymerised directly on the MXene surface. It facilitates charge transfer between the molecular orbitals of the MXene and the polymer. This creates conductive channels and widens the space between MXene layers. This method greatly increases the electrical conductivity and capacitance of the resulting composites by increasing the layer spacing and improving the flow of electrons and ions. In situ polymerisation is used to make reinforced composites with different polymers, such as (Jain et al., 2026; L. Zhou et al., 2025):

- **Thermosets & Thermoplastics:** Polyurethane (PU), epoxy resin (EP), and PMMA. In epoxy, the polymer chains penetrate the MXene layers, strengthening the overall chemical structure during curing.

- **Conductive Membranes:** Electrophoresis deposition is the first phase in making $\boldsymbol{Ti_3C_2T_x/PPy}$ hybrid membranes. The second step involves injecting and polymerising pyrrole. This method is especially promising for energy storage because it enables the fabrication of thin, solid-state supercapacitors with excellent electrochemical performance and cycle stability.

4.4.4 Hot press

A high-powered mixer at controlled temperatures mixes MXene with a molten polymer matrix. Then, heat pressing is used to turn this mixture into the final composite material. The main benefit of this method is that it increases the materials' thermal stability, raising their breakdown temperatures significantly.

Hot pressing is superior to other methods because it outperforms solution-based approaches, especially for polymers that don't dissolve or disperse MXene flakes.

Compatible Polymers: This method has worked well with a wide range of polymers, including PU, PS, PANI, PVDF, UHMWPE, and LLDPE. (Munshi et al., 2026).

4.4.5 Layer-by-layer (LBL) assembly

The Layer-by-layer (LBL) assembly method involves the sequential deposition of layers of Ti_3C_2Tx MXenes and polymers onto a substrate. Spray deposition, spin coating, and dip coating can regulate the MXene-to-polymer ratio and thickness by process repetition. In a specific application, MXene was combined with tris(2-aminoethyl)amine (TAEA) to create multilayer structures, referred to as (MXene/TAEA)n, using vacuum-assisted layer-by-layer self-assembly. We made solutions of Ti_3C_2Tx MXene and TAEA at a concentration of $1\ g/L$ were sprayed onto porous substrates that were held in place in a vacuum system. The assembly process consisted of spraying, washing, and depositing layers in turns until the desired thickness was reached. We also used a quick-LBL method on bigger $3D$ shapes, such as CNF aerogels and melamine foam. Another study looked at LBL assembly for polyaniline nanofibers and Ti_3C_2Tx MXene electrodes to improve electrochemical energy storage. (Wang et al., 2022).

4.4.6 Electrospinning method

The electrospinning method is a flexible, scalable approach for producing MXene-polymer nanocomposite membranes. This method uses a high voltage to draw a polymer solution into fine jets, which then harden into nanofibers. Then, these nanofibers are collected on a rotating drum, forming a continuous membrane with a large surface area and strong mechanical properties. The electrospinning process enables the integration of MXene into polymer matrices, thereby improving charge transport, signal sensitivity, and mechanical compliance. This makes it useful for a wide range of uses, including flexible sensors and biomedical devices.

To prepare MXene-polymer composites for electrospinning, a polymer solution must first be prepared. After that, the polymer solution is sonicated to ensure that the MXenes are equitably distributed. Subsequently, electrospinning will be employed to fabricate MXene-functionalized composites using this MXene-polymer solution (Mayerberger et al., 2018). Key factors, such as the choice of polymer, the amount of MXene incorporated, the selection of solvents, and adjustments to electrospinning parameters, play a critical role in determining the properties of the resulting MXene- integrated electrospun composites (Khadem et al., 2025a).

4.4.6.1 Selection of Polymer

The choice of polymer is crucial in shaping the shape of MXene-based electrospun nanocomposites. Various polymers, including polyvinylidene fluoride (PVDF) (Dallaev et al., 2022), polyurethane (PU) (S. Wu et al., 2025), polyacrylonitrile (PAN) (Wafaa Kh Al-Musawy et al., 2026), nylon-6 (Massey, 2007), poly(vinyl alcohol) (PVA) (Liang et al., 2024), have been used for wastewater treatment (Jain et al., 2026). The selected polymer influences the viscosity, crystallinity, conductivity, and fiber diameter of the resulting composites. For example, research by Mayerberger et al. (Mayerberger et al., 2017) demonstrated that the Ti_3C_2Tx/poly(ethylene oxide) (PEO) composite achieved a significant decrease in fiber diameter due to its high conductivity and viscosity. In contrast, the PVA-Ti_3C_2Tx composite showed limited conductivity and resulted in thicker fibers

due to stronger hydrogen bonding. Other combinations, like PAA-Ti_3C_2Tx and alginate/PEO-Ti_3C_2Tx, displayed varying effects on fiber morphology based on their interactions and solution properties. This underscores the importance of selecting the appropriate polymer for effective fabrication of electrospun MXene/polymer composites (Khadem et al., 2025b).

4.4.6.2 Loading MXene

The quantity of MXene nanosheets incorporated into the polymer solution during electrospinning significantly impacts the properties and performance of the nanofibers (Khadem et al., 2025b; Pant et al., 2023a; Renkler et al., 2025). A study by Gao et al. (Gao et al., 2019b) investigated the impact of varying MXene loading $(0, 25, 50, 100, \text{and } 400\ \mu g)$ on PAN-Ti_3C_2Tx MXene nanofibers. The resulting fibers were labeled P@M-1 to P@M-4. At lower MXene loadings (P@M-1 and P@M-2), the fibers had an average diameter of $122\ nm$ and $116\ nm$, respectively, and exhibited a smooth, bead-free structure. However, at a higher loading of $400\ \mu g$ (P@M-4), the diameter increased to $120\ nm$ with a wider distribution, and the fibers became rough with noticeable bead formations. The alteration was ascribed to the aggregation of MXene nanosheets, indicating that modest MXene loading can improve fibre structure, whereas excessive loading may lead to uneven fibres with variable diameters.

4.4.6.3 Solvent Selection

The choice of solvent used in the process has a big effect on how MXene-based nanofibers are made and what they are like (Jain et al., 2026). It is important to completely dissolve the polymer and mix the MXene nanosheets into a uniform solution. This is especially true because MXenes have a low zeta potential in water at neutral pH, and many polymers do not dissolve in water (Khadem et al., 2025c). To tackle this issue, various polar organic solvents, including DMF, acetone, water, formic acid, tetrahydrofuran (THF), and sodium dodecyl sulphate (SDS), have been used to prepare electrospinning solutions (Xu et al., 2024).

The boiling point and vapour pressure of the solvent affect the solution's viscosity, which, in turn, alters the shape of the fibres and the way the jet forms (Shlapakova et al., 2026). A solvent with higher conductivity makes the fibres more uniform, and the right viscosity range $(1425 - 2375\ cP)$ makes sure that the flow is smooth during the electrospinning process. The solvent's rate of evaporation is also very important; the faster it evaporates, the less solvent is left over, which means fewer beads form and the fibre structure gets better (Higashi et al., 2020; Yu and Tan, 2025).

Choosing the right solvents is important not only for ensuring MXene mixes evenly with the polymer matrix, but also for preventing clumping (Gholami et al., 2024). In addition to technical issues, the safety and environmental effects of solvents must come first. Choosing solvents that are low in toxicity and volatility can reduce the risk of skin irritation and breathing problems. It can also reduce the need for extensive ventilation and lower air emissions. Also, solvents that release fewer toxic vapours are simpler to contain and dispose of, which is consistent with the principles of green chemistry and safety regulations (Mansour and Bedair, 2025).

4.4.6.4 Parameters of Electrospinning

Identifying the ideal electrospinning parameters for MXene/polymer composites is crucial to improve fibre shape, electrical conductivity, and mechanical flexibility, all of which are vital for flexible sensing applications. Key parameters include nozzle gauge $(21 - 24\ G)$, electric field strength $(10 - 30\ kV)$, tip-to-collector distance $(10 - 20\ cm)$, flow rate $(0.2\ \mu L/s\ to\ 2\ mL/h)$, collector type, relative humidity $(RH\ 30\% - 97\%)$, and temperature (typically $25\ °C$) (Abdul-Hussein et al., 2024; Yan et al., 2022).

The nozzle gauge is selected to ensure uniform fiber formation and stable jet ejection. Electric field strength strongly influences fiber continuity, with higher voltages $(> 20\ kV)$ yielding finer nanofibers suitable for strain and pressure sensing due to improved conductivity. Moderate voltages $(\sim 15\ kV)$ help maintain uniform fiber thickness (SalehHudin et al., 2021).

The distance from the tip to the collector impacts how quickly the solvent evaporates and how fibres are deposited. Shorter lengths produce thicker layers, whereas longer lengths produce fewer flaws. Flow rate affects fiber diameter and porosity: lower rates produce ultrafine, porous fibers ideal for capacitive sensing, while higher rates form uniform, conductive networks for strain and humidity sensing (Yousefzadeh and Ramakrishna, 2017).

Collector type affects fiber orientation and mechanical flexibility; stationary collectors yield random deposition, resulting in isotropic conductivity, whereas rotating drums align fibers for filtration membranes. Relative humidity affects fiber morphology: lower levels produce smooth fibers, while higher levels enhance sensitivity through nanoporosity. Maintaining a consistent temperature is essential to prevent phase separation that can degrade properties (Alfaro De Prá et al., 2017).

Electrospun composites functionalised with MXene can achieve enhanced environmental stability, mechanical flexibility, and electrical conductivity by systematically modifying electrospinning conditions. This makes them appropriate for advanced applications in flexible electronics, environmental monitoring, and human motion sensing (Li et al., 2024; W. Wu et al., 2025a).

5. MORPHOLOGICAL EVOLUTION AND SURFACE WETTABILITY

The surface wettability and morphological evolution of MXenes are of great significance for their applications in various fields. The structural structure of the membrane is significantly altered by the incorporation of MXene loading levels (Huang et al., 2025).

5.1 Effect of MXene Concentration on Membrane Porosity

The incorporation of MXenes into electrospun polymeric membranes can remarkably alter the morphology of the membrane and the wettability of the surface, which are closely related to the filtration performance

- Low Loading (e.g. 0.05 wt%): The fibres maintain a smooth, continuous cylindrical profile. Nanoclusters are sparsely present and cause only minor changes to the baseline polymer topography.

- Optimal Loading (e.g. 0.10 wt%): Homogeneous decoration of the fibre surfaces with a distinct, crystalline-like nanocluster topography. The fully retained interconnected 3D porous structure avoids the blockage of pores and increases the specific surface area drastically.

- High Loading (e.g., 0.15 wt%): The high MXene content can lead to aggregation of the nanosheets at the fibre junctions and in localised areas of the membrane. This aggregation can block pores, disturb the fibrous matrix, and decrease hydraulic permeability, thus preventing flow performance even at higher filler concentrations (Al-Okaidy and Waisi, 2023; Ruiz Rocha et al., 2023; W. Wu et al., 2025b).

So, managing the amount of MXene is important to ensure the final membrane has a good balance of structure, holes, and how well it allows things to pass through.

5.2 Surface Wettability Transformations

In many cases, pristine polymeric membranes exhibit low fouling resistance or moderate hydrophobicity. The MXene molecular signature is rich in polar hydrophilic groups $(-OH, =O)$. These groups hydrogen bond strongly to water. These groups form strong hydrogen bonds with water (Thakur et al., 2026). Under water they form a thick, stable layer of hydration (Helal et al., 2024). This shield is active and prevents direct adhesion of organic contaminants and oil drops to the polymeric strands. Surface wettability of MXenes is one of the important factors for their applications in various industries (Malaki and Varma, 2023). The hydrophilic nature of MXenes allows processing to low contact angles, a prerequisite for their application in nano-hybrid structures and composite materials (Feng et al., 2022b). Surface terminations of MXenes can affect their wettability and properties such as stability and work function can be tuned by the surface terminations (Pang et al., 2024).

6. PERFORMANCE IN WATER TREATMENT APPLICATIONS

MXene-based polymer nanocomposite membranes have attracted significant attention for wastewater treatment due to their ability to remove a range of contaminants across multiple categories, including dyes, pharmaceuticals, and heavy metals. Traditional polymeric membranes have limitations, including limited selectivity, susceptibility to fouling, and inadequate removal of emerging pollutants, despite their widespread application. Adding MXenes is a complex solution, as they are highly hydrophilic, negatively charged, and functionalized with surface groups ($–OH$, $–O$, $–F$) that facilitate adsorption and rejection of contaminants (Du et al., 2025).

6.1 pharmaceuticals

New contaminants, including antibiotics and hormone-altering compounds, are increasingly being detected in water. MXene-based nanocomposites have demonstrated potential for rejecting compounds such as tetracycline and ibuprofen via electrostatic interactions and hydrogen bonding. Their antibacterial action also stops biofilm development, which is one of the biggest problems with standard membranes (Ahmaruzzaman, 2022).

MXene membranes show strong promise for pharmaceutical wastewater treatment because their regular slit-shaped nanochannels, tunable interlayer spacing, functional groups like $-OH, -COOH, or\ -NH_2$ enable strong electrostatic interactions, and a 2D lamellar structure enables efficient antibiotic separation via size-exclusion and electrostatic interactions. (Munshi et al., 2026). A study examined how specific drugs, both anionic and cationic, bind to MXene. At $pH\ 7$, it was shown that cationic pharmaceutical compounds can adsorb up to 58.7 mg/g. Using sonicated MXene, which can adsorb $214\ mg/g$ at a frequency of $28\ kHz$, also made it easier to get rid of cationic medicinal compounds. It is recommended to do further research on the production of $NH_2 -$ functionalized MXene to make it easier for anionic medicinal chemicals to stick to it (Ihsanullah, 2022).

6.2 Heavy metals

MXene composites facilitate heavy metal removal through various mechanisms, including filtration, adsorption, electrostatic interactions, and ion exchange, effectively capture and eliminate pollutants such as mercury (Hg^{2+}), lead (Pb^{2+}), chromium (Cr^{6+}), copper (Cu^{2+}), and cadmium (Cd^{2+}) (Munshi et al., 2026). Numerous studies have shown that they can remove more than 95% of pollutants from industrial wastewater, indicating they are well-suited for this purpose. Also, MXenes have a two-dimensional lamellar structure that allows water to pass easily and facilitates ion sieving. Textile effluents containing synthetic dyes remain difficult to treat using conventional methods (Sun et al., 2024b). For example,

MXene composites modified with poly(m-phenylenediamine) (PmPD) efficiently remove Cr^{6+} with approximately 100% elimination and a maximum adsorption capacity of $540.47\ mg/g$ within $2\ hours$ at $27\ °C$ and $pH\ 2$. Similarly, MXene/ALG composites exhibited effective removal of Pb^{2+}, achieving an adsorption capacity of $382.7\ mg/g$ and a removal efficiency of 86.7% within $15\ minutes$ at $25\ °C$ and $pH\ 6$ (Munshi et al., 2026). Zhou et al. (2025) created a collagen-based aerogel modified with MXene@polydopamine and oxidised sodium alginate (MPAC) (J. Zhou et al., 2025). At initial concentrations of $30, 70$, and $100\ mg/L$, the aerogel exhibited $Cr(VI)$ adsorption capacities of $80.73, 100.80$, and $112.86\ mg/g$, respectively. The process was spontaneous and endothermic, adhering to the Freundlich isotherm model. This means that the surface was not uniform and had a strong attraction to hexavalent chromium. Also, the MPAC aerogel showed that it could use solar energy to evaporate water, which combined pollutant removal with efficient use of solar energy.

6.3 Dyes

Because of industrialisation, water pollution has worsened, making wastewater treatment even more important. Numerous MXene-based polymer composites exhibit exceptional adsorption properties, with certain compounds capable of eliminating a diverse array of hues (Munshi et al., 2026). Cationic dyes, such as crystal violet (CV) and methylene blue (MB), are firmly rejected by MXene–polymer hybrids (over 90%) due to size exclusion, $\pi - \pi$ interactions, and electrostatic repulsion (Jain et al., 2026).

For instance, MXene/graphene oxide (GO) composites have attained a Chrysoidine G (CG) removal efficacy of approximately 97% with a flow of $71.9\ L/m^2\ h$. Conversely, MXene/GO/Nylon composites exhibit exceptional effectiveness in the removal of methylene blue (MB), achieving a removal efficiency of 97% and a substantial water flux of $82.5\ L/m^2\ h$. The adsorption studies were performed under optimal conditions, comprising an initial MB concentration of $10\ mg/L$, a contact duration of 30 minutes, and a temperature of $25\ °C$ (Han and Wu, 2019).

Charge-based attraction and pore-size exclusion control how well MXene–polymer membranes remove dye. Both of these can be changed by changing the chemicals and the nanostructure. Because they carry a negative charge on their surfaces, MXenes can attract cationic dyes such as methylene blue (MB). Functional groups like $-SO_3\ H$ or $-NH_2$ can strengthen the binding and increase the spacing between layers. Adding polymers such as chitosan (CTS) or polyamide (PA) makes the material more stable and less likely to break, while adding nanoparticles can control the interlayer spacing to keep the material permeable without compromising its ability to reject dye (Jain et al., 2026).

Natural Resources for Human Health
eISSN: 2583-1194

6.4 Oil-Water Emulsion Separation

Industrial wastewater effluents often contain pollutants that pose significant long-term hazards to human health and environmental integrity; therefore, these pollutants must be removed before discharge. MXene nanosheets have been proposed as promising materials for membrane nanofiltration to improve the separation of oil–water mixtures (AlHadithy et al., 2024). Researchers developed novel TA-ZIF-8@MXene membranes that integrate tannic acid-modified ZIF-8 nanoparticles to mitigate water barrier resistance. These membranes exhibited favourable flux recovery ratios. The use of hydrophilic TA-ZIF-8 nanoparticles improved water permeability, making the membrane surface exceptionally hydrophilic and oleophobic (Zeng et al., 2022). Furthermore, composite membranes of 2D Na-Bentonite@MXene with switchable wettability have been produced, showing rejection ratios of 96% and recovery rates of 86% after eight cycling tests. These membranes may alternate between hydrophilic/hydrophobic and hydrophobic/oleophobic surfaces based on the presence of water or oil (Zhang et al., 2023).

6.5 Desalination (salt rejection, permeability)

MXene-based membranes have attracted substantial interest for desalination due to their hydrophilic functional groups, adjustable interlayer spacing, and two-dimensional structure, which collectively enhance water transport and ion rejection. Numerous MXene membrane designs have been proposed in recent research to enhance desalination efficiency. These consist of thin-film nanocomposite membranes, capacitive deionisation devices, and photothermal distillation (Jabeen et al., 2025). In 2024, Usman et al. developed sulfonated MXene-based thin-film nanofiltration membranes using interfacial polymerisation using APIP and DABSA monomers (Jain et al., 2026). Zhu et al. concurrently synthesised Ag@MXene heterojunction membranes for photothermal membrane distillation (PMD) (Zhu et al., 2025). MXene nanosheets made the material more hydrophilic (contact angle $\sim 24°$), more resistant to fouling, and capable of rejecting more than 93% of Na_2SO_4 and $MgSO_4$, which is better than regular TFN membranes. The plasmonic coupling effect greatly improved the efficiency of solar-thermal conversion (77%) and the flow of freshwater, showing that it is possible to use this technology to desalinate seawater in a way that saves energy. Outdoor tests showed a peak flow of $21.53\ kg\ m^{-2}\ h^{-1}$ and a salt rejection rate of 99.95% when there was one sun shining.

Notwithstanding its promise, research on ion-selective separation remains in its infancy. There are currently very few published studies that use selective MXene membranes to extract electricity using a salinity gradient or to sieve salts and heavy metals. Several monovalent and multivalent ionic species were able to flow through the lamellar MXene membranes, indicating a decrease in penetration rate in the following order: $Na^+ > Li^+ > K^+ > Ca^{2+} > Ni^{2+} > Mg^{2+} > Al^{3+}$.

Research indicates the formation of non-swelling MXene membranes by the intercalation of Al^{3+} ions. Swelling is inhibited by robust contacts between Al^{3+} ions and the oxygen functional groups that finish the MXene surface. The membranes possess a thickness of $1.1\ \mu m$, exhibit significant NaCl rejection rates (about $89.5\% - 99.6\%$), demonstrate rapid water fluxes (around $1.1 - 8.5\ L/m\text{^}2\ h$), and maintain outstanding non-swelling stability in aqueous solutions for up to 400 hours. These membranes can be readily fabricated using fundamental filtration and ion-intercalation techniques, suggesting their scalability (Munshi et al., 2026).

7. CURRENT CHALLENGES AND FUTURE PERSPECTIVES

The MXene-based membranes are facing some challenges in the wastewater treatment, including permeability-selectivity trade-off, fouling, oxidation, and swelling. Challenges limit its effectiveness in actual applications. However, further research and development, innovative design methods and a better understanding of separation processes are important to solving these problems (Ghanbari and Nazarzadeh Zare, 2024). Future work will involve exploring new membrane topologies to increase operational capacity and optimising the mechanical, optical and electrical properties of MXene to improve its performance in a variety of applications (Sun et al., 2024b).

1. **Chemical Stability in the Long Term:** MXene-based membranes show great promise for short-term use in labs, but they require careful testing for stability before they can be used on a large scale and for extended periods (Sun et al., 2024b). Environmental factors, such as exposure to chlorine, changes in pH, and oxidative degradation, significantly affect how long something lasts. For example, studies have shown that $Ti_3C_2T_x$ oxidises in water, making TiO_2, which makes membranes less conductive and selective (Qu et al., 2021). There are also concerns about residual fluoride ions from HF-based etching, which

could harm performance and the environment (Fu et al., 2026). Using green etchants, such as LiF/HCl or molten salts, and antioxidants, such as ascorbic acid, has been suggested to make materials more resistant to oxidation.

2. **Mechanical Resistance to Pressure:** Electrospun mats tend to be compacted under high pressure in continuous operations. Phases of crosslinking or heat treatment (stabilisation) are necessary to retain the geometric porosity on a long term. In numerous membrane-based separation processes, MXene has exhibited remarkable flexibility, hydrophilic surface characteristics, and superior mechanical strength. Moreover, enhanced mechanical strength can guarantee that the improved MXene membranes perform more effectively in separation processes (Pan et al., 2026). Significantly, enhanced mechanical performance is directly associated with steady operation in high-pressure filters. For instance, the enhanced stiffness observed in materials like MXene/PLA, attaining levels of $164.99\ MPa$, prevents membranes from being compressed under high water pressure during processes such as nanofiltration or reverse osmosis (Munshi et al., 2026).

3. **Scalability and Economic Feasibility:** The manufacturing of single-layer MXene is constrained to bulk methods because to the utilisation of hazardous etching chemicals (HF). The advancement of environmentally sustainable and scalable exfoliation techniques is essential to meet the requirements of sustainable industrial production. A comprehensive assessment of the stability and scalability of MXene-based composite membranes highlights the need for additional long-term research and industrial pilot trials, which are currently lacking. Therefore, thorough examinations focused on lifecycle stability evaluation and module-level verification are crucial for validating MXene membranes as appropriate materials for industrial use (Cui et al., 2023).

8. CONCLUSION

Electrospun nanofiber membranes with MXene are a very promising platform for improved water filtration. The long-standing three-dimensional fibrous network provides limited structural resistance, whereas the unique surface chemistry of two-dimensional MXenes enhances Superhydrophilicity and excellent anti-fouling performance. Systematic control of solution parameters and the incorporation of nanomaterials can lead to improvements in the well-established trade-off between water flux and pollutant removal, opening the door to next-generation environmental remediation technology.

ACKNOWLEDGEMENTS

The authors would like to thank the Department of Biochemical Engineering, Faculty of Al-Khwarizmi Engineering, Baghdad University, and the Scientific Research Commission for providing the technical support to complete the scientific review.

AUTHOR CONTRIBUTIONS

Israa M. Rashid: Methodology, Laboratory Analysis.

Mustafa H. Al-Furaiji: Data Curation, Formal Analysis.

Alaa Kareem Mohammed: Supervision, Writing—Review & Editing.

CONFLICT OF INTEREST

The authors declare that there is no conflict of interest.

ETHICS STATEMENT

Ethical approval was not required for this study.

DATA AVAILABILITY STATEMENT

The data that support the findings of this study are available from the corresponding author upon reasonable request.

FUNDING INFORMATION

This research received no specific grant from any funding agency in the public, commercial, or not-for-profit sectors.

CONFLICT OF INTEREST

The authors declare no conflict of interest.

Natural Resources for Human Health
eISSN: 2583-1194

Table 1. MXenes synthesis and summarizes their advantages and disadvantages

Synthesis route	Main principle	Advantages	Limitations	Relevance to membrane preparation	Ref.
HF etching	Direct chemical removal of the A-layer using HF	High etching efficiency, well established	Highly toxic and unsafe	Suitable for laboratory-scale preparation, but environmentally limited	(Patial et al., 2025)
LiF/HCl etching (MILD)	In situ generation of HF from fluoride salt and acid	Safer than direct HF, controllable etching	Still fluoride-based	Widely used for preparing high-quality MXenes for composites	(Huang and Han, 2023)
Hydrothermal etching	Alkali-assisted etching under elevated temperature and pressure	HF-free, relatively scalable	Requires harsh conditions and long reaction time	Promising for safer synthesis, though less common	(Abid et al., 2024)
Electrochemical etching	Anodic removal of the A-layer under applied potential	Fluoride-free, controllable surface chemistry	Risk of over-etching, process optimization required	Attractive for cleaner MXene production	(Nouseen and Pumera, 2025)
Molten-salt etching	Lewis-acid-mediated etching using molten salts	Tunable terminations, new surface chemistries	More complex processing	Useful for advanced functional membranes	(Wang et al., 2023)

Table 2. Various MXene -Polymer Nanocomposites membrane for water treatment.

MXene	Polymers	Performance	References
Ti_3C_2Tx	Polyvinylidene fluoride (PVDF)	over 99% growth inhibition of Escherichia coli (E. coli) and Bacillus subtilis (B. subtilis)	(Rasool et al., 2017)
Ti_3C_2Tx	PAN / Poly (vinyl alcohol) (PVA)	Adsorption capacity 100–500 (Pb^{2+}, Cu^{2+}, Cr^{6+})	(Fatima et al., 2022)
Ti_3C_2Tx	poly (arylene ether nitrile) (PEN)	15 ppm MB, MO, CV, and MeB solutions achieved 92.31%, 93.50%, 98.06%, and 99.30% within 60 min, respectively	(Feng et al., 2022b)
Ti_3C_2Tx	ZnO/poly(arylene ether nitrile)	separating various oil emulsions separation efficiency (>99.4%), even in high-temperature and salty environments	(Sun et al., 2022)
(Ti_3C_2Tx) MXene @Ag	poly (arylene ether nitrile) (PEN)	Different oil–water emulsions rejection rate (99.13%)	(Feng et al., 2022a)
Ti_3C_2Tx	PAN	flux recovery ratio of about 80%	(Imsong and Dhar Purkayastha, 2023)

REFERENCES

[1] Abdul-Hussein, S.T., Alsalhy, Q.F., Al-Furaiji, M.H., Russo, F., Chiappetta, G., Di Luca, G., Figoli, A., 2024. Arabian Journal of Chemistry 17, 105475.
[2] Abid, M.Z., Rafiq, K., Aslam, A., Jin, R., Hussain, E., 2024. J. Mater. Chem. A 12, 7351–7395.
[3] Abraham Swu, Y., Dhar Purkayastha, D., 2025. Applied Surface Science 680, 161365.
[4] Ahmadi Bonakdar, M., Rodrigue, D., 2024. Macromol 4, 58–103.
[5] Ahmaruzzaman, M., 2022. RSC Advances 12, 34766–34789.
[6] Al-Musawy, Wafaa Kh., Al-Furaiji, M.H., Hassoon, G.S., Shehan, A., 2026. Environmental Progress \& Sustainable Energy n/a, e70418.
[7] Al-Musawy, Wafaa Kh, Waisi, B.I., Al-Furaiji, M.H., Shehan, A., Jahangiri, M., 2026. Al-Khwarizmi Engineering Journal 22, 1–13.
[8] Al-Okaidy, H.S., Waisi, B.I., 2023. Baghdad Science Journal 20, 1433–1441.
[9] Alfalluji, A.L., 2025. 37899–37907.
[10] Alfaro De Prá, M.A., Ribeiro-do-Valle, R.M., Maraschin, M., Veleirinho, B., 2017. Materials Letters 193, 154–157.
[11] AlHadithy, Z.E., AbdulRazak, A.A., Al-Ghaban, A.M.H.A., Alsalhy, Q.F., Meskher, H., Al-Juboori, R.A., Katibi, K.K., Lawal, D.U., 2024. Advancements in Water Treatment with MXene-Enhanced Membranes: A Review of Current Progress and Future Directions, Water, Air, and Soil Pollution. Springer International Publishing.
[12] Antony Jose, S., Price, J., Lopez, J., Perez-Perez, E., Menezes, P.L., 2025. Materials 18.
[13] Bachs-Herrera, A., Yousefzade, O., Del Valle, L.J., Puiggali, J., 2021. Applied Sciences (Switzerland) 11, 1–39.
[14] Bisht, N., Jaiswal, S., Vishwakarma, J., Gupta, S.K., Yeo, R.J., Sankaranarayanan, S.K.R.S., Dhand, C., Dwivedi, N., 2024. Chemical Engineering Journal 498.
[15] Bonakdar, M.A., Rodrigue, D., 2024. 58–103.
[16] Buzgo, M., Mickova, A., Rampichova, M., Doupnik, M., 2018. 11 - Blend electrospinning, coaxial electrospinning, and emulsion electrospinning techniques, in: Focarete, M.L., Tampieri, A. (Eds.), Core-Shell Nanostructures for Drug Delivery and Theranostics, Woodhead Publishing Series in Biomaterials. Woodhead Publishing, pp. 325–347.
[17] Carroll-Bassham, H., Brettmann, B.K., 2024. MRS Communications 14, 1416–1423.
[18] Castellanos-Espinoza, R., Arjona, N., España-Sánchez, B.L., 2025. Advances in Electrospun Nanostructured Membranes for Wastewater Treatments: Challenges and Opportunities, Environmental Science and Engineering. Springer Nature Switzerland.
[19] Chen, Y., Cheng, J., Wang, A., Liu, C., Yan, H., Qiu, Y., Wang, Z., Chu, P.K., Luo, Y., 2024. Inorganic Chemistry Communications 159, 111793.
[20] Crini, G., Lichtfouse, E., Wilson, L.D., Morin-Crini, N., 2019. Environmental Chemistry Letters 17, 195–213.
[21] Cui, J., Li, F., Wang, Y., Zhang, Q., Ma, W., Huang, C., 2020. Separation and Purification Technology 117116.
[22] Cui, Y., Zhu, J., Tong, H., Zou, R., 2023. iScience 26.
[23] Dallaev, R., Pisarenko, T., Sobola, D., Orudzhev, F., Ramazanov, S., Trčka, T., 2022. Polymers 14.
[24] Damptey, L., Jaato, B.N., Ribeiro, C.S., Varagnolo, S., Power, N.P., Selvaraj, V., Dodoo-arhin, D., Kumar, R.V., Sreenilayam, S.P., Brabazon, D., Thakur, V.K., Krishnamurthy, S., 2022. 2100120.
[25] Date, M., Jaspal, D., 2024. Sustainable Water Resources Management 10, 90.
[26] Dhamodharan, D., Al-Harthi, M.A., Ramya, B., Bafaqeer, A., Alam, F., 2024. Journal of Environmental Chemical Engineering 12, 112316.
[27] Du, Y., Yu, J., Chen, B., Zhu, X., 2025. Environ. Sci.: Nano 12, 150–188.
[28] Fatima, H., Seo, J.-D., Kim, J., Park, M., 2022. Journal of Porous Materials 29, 111–117.
[29] Feng, Q., Zhan, Y., Yang, W., Dong, H., Sun, A., Li, L., Chen, X., Chen, Y., 2022a. Separation and Purification Technology 298, 121635.
[30] Feng, Q., Zhan, Y., Yang, W., Sun, A., Dong, H., Chiao, Y.H., Liu, Y., Chen, X., Chen, Y., 2022b. Journal of Colloid and Interface Science 612, 156–170.
[31] Feng, Y., Wang, Hui, Xu, J., Du, X., Cheng, X., Du, Z., Wang, Haibo, 2021. Journal of hazardous materials 416, 125777.
[32] FitzPatrick, J., Gogotsi, Y., 2025. MRS Bulletin 50, 1351–1363.
[33] Fu, B., Kong, N., Ren, L.F., Shao, J., 2026. Separation and Purification Technology 382, 135737.
[34] Gao, X., Li, Z., Xue, J., Qian, Y., Zhang, L., Caro, J., Wang, H., 2019a. 586, 162–169.

[35] Gao, X., Li, Z.K., Xue, J., Qian, Y., Zhang, L.Z., Caro, J., Wang, H., 2019b. Journal of Membrane Science 586, 162–169.
[36] Ghanbari, R., Nazarzadeh Zare, E., 2024. Coordination Chemistry Reviews 518, 216089.
[37] Gholami, T., Seifi, H., Dawi, E.A., Pirsaheb, M., Seifi, S., Aljeboree, A.M., Hamoody, A.H.M., Altimari, U.S., Ahmed Abass, M., Salavati-Niasari, M., 2024. Materials Science and Engineering: B 304, 117370.
[38] Hada, V., Malvi, D., Mili, M., Khan, M.M., Chaturvedi, G., Hashmi, S.A.R., Srivastava, A.K., Verma, S., 2022. Materials Advances 3, 7445–7462.
[39] Han, R., Wu, P., 2019. J. Mater. Chem. A 7, 6475–6481.
[40] Helal, M.I., Sinopoli, A., Gladich, I., Tong, Y., Alfahel, R., Gomez, T., Mahmoud, K.A., 2024. J. Mater. Chem. A 12, 30729–30742.
[41] Higashi, S., Hirai, T., Matsubara, M., Yoshida, H., Beniya, A., 2020. Scientific Reports 10, 13427.
[42] Hou, K., Zhou, H., Zhu, K., Xie, C., Liu, S., He, Y., Zhu, X., Wu, M., Huang, T., 2023. Carbohydrate Polymer Technologies and Applications 5, 100278.
[43] Huang, P., Han, W.-Q., 2023. Nano-Micro Letters 15, 68.
[44] Huang, W., Wang, J., Lai, W., Guo, M., 2025. Molecules 30.
[45] Ihsanullah, I., 2022. Journal of Environmental Chemical Engineering 10, 107381.
[46] Imsong, R., Dhar Purkayastha, D., 2023. Separation and Purification Technology 306, 122636.
[47] Jabeen, T., Rashid, M., Haider, S., Azam, M., 2025. Journal of Hazardous Materials Advances 19, 100814.
[48] Jabur, A.R., Abbas, L.K., Moosa, S.A., 2017. Al-Khwarizmi Engineering Journal 13, 84–93.
[49] Jain, H., Singh, L., Shrivastava, A., Paul, M., Horo, H., Samuel, H.S., 2026. Next Materials 10, 101574.
[50] Ji, D., Lin, Y., Guo, X., Ramasubramanian, B., Wang, R., Radacsi, N., Jose, R., Qin, X., Ramakrishna, S., 2024. Nature Reviews Methods Primers 4, 1.
[51] Ji, K., Liang, Z., Wang, P., Li, Z., Ma, Q., Su, X., 2024. Chemical Engineering Journal 495, 153598.
[52] Jin, S., Guo, Y., Wang, F., Zhou, A., 2023. MRS Bulletin 48, 245–252.
[53] Jun, B.M., Jang, M., Park, C.M., Han, J., Yoon, Y., 2020. Nuclear Engineering and Technology 52, 1201–1207.
[54] Kadhom, M., Albayati, N., Alalwan, H., Al-Furaiji, M., 2020. Sustainable Chemistry and Pharmacy 16, 100259.
[55] Kadhom, M., Kalash, K., Al-Furaiji, M., 2022. Chemosphere 290, 133256.
[56] Kamto, M., 2016. International Law Commission 38067, 1–47.
[57] Kamysbayev, V., Filatov, A.S., Hu, H., Rui, X., Lagunas, F., Wang, D., Klie, R.F., Talapin, D. V, 2020. Science 369, 979–983.
[58] Khadem, A.H., Anik, H.R., Limon, G.M., Rabbani, M., Rafi, A.S., Mim, I.K., Rahman, H., Alam, F. Bin, Islam, K., Munira, S.S., Islam, T., Uddin, M., Mony, H., 2025a.
[59] Khadem, A.H., Anik, H.R., Limon, M.G.M., Rabbani, M., Rafi, A.S., Mim, I.K., Rahman, M.H., Alam, F. Bin, Islam, M.K., Munira, S.S., Islam, M.T., Uddin, M., Mony, H., 2025b. ACS Applied Nano Materials 8, 16231–16259.
[60] Khadem, A.H., Anik, H.R., Limon, M.G.M., Rabbani, M., Rafi, A.S., Mim, I.K., Rahman, M.H., Alam, F. Bin, Islam, M.K.T., Munira, S.S., Islam, M.K.T., Uddin, M., Mony, H., Limon, G.M., Rabbani, M., Rafi, A.S., Mim, I.K., Rahman, H., Alam, F. Bin, Islam, K., Munira, S.S., Islam, T., Uddin, M., Mony, H., Limon, M.G.M., Rabbani, M., Rafi, A.S., Mim, I.K., Rahman, M.H., Alam, F. Bin, Islam, M.K.T., Munira, S.S., Islam, M.K.T., Uddin, M., Mony, H., 2025c. ACS Applied Nano Materials 8, 16231–16259.
[61] Kiran, H., Ali, A.B.M., Ashraf, R., Tahir, M.B., Nasir, M., Hasnain, N., Ullah, M.F., Abduvalieva, D., Batool, N., 2025. Journal of Inorganic and Organometallic Polymers and Materials 35, 9565–9578.
[62] Kumar, S., Taunk, M., 2024. Materials Today Physics 46, 101483.
[63] Kumar, Sunil, Zain Mehdi, S.M., Taunk, M., Kumar, Sanjeev, Aherwar, A., Singh, S., Singh, T., 2025. Journal of Materials Chemistry A 13, 11050–11113.
[64] Li, X., Wang, S., Zheng, M., Ma, Z., Chen, Y., Deng, L., Xu, W., Fan, G., Khademolqorani, S., Banitaba, S.N., Osman, A.I., 2024. Nanoscale Horizons 9, 1703–1724.
[65] Liang, X., Zhong, H.-J., Ding, H., Yu, B., Ma, X., Liu, X., Chong, C.-M., He, J., 2024. Polymers 16.
[66] Liu, L., Zschiesche, H., Antonietti, M., Gibilaro, M., Chamelot, P., Massot, L., Rozier, P., Taberna, P., Simon, P., 2023. Advanced Energy Materials 13.
[67] Liu, W., Walker, G., Price, S., Yang, X., Li, J., Bunt, C., 2021. Pharmaceutics 13.

[68] Mailley, D., Hébraud, A., Schlatter, G., 2021. Macromolecular Materials and Engineering 306.
[69] Malaki, M., Varma, R.S., 2023. Nano-Micro Letters 15, 116.
[70] Mannafi, A.S.M., Habib, K., Ali, S.A., Younas, M., Bakthavatchalam, B., Saha, B.B., 2025. Results in Engineering 27, 107027.
[71] Mansour, F.R., Bedair, A., 2025. Sustainable Chemistry and Pharmacy 47, 102157.
[72] Massey, L.K., 2007. The Effects of UV Light and Weather on Plastics and Elastomers 117–125.
[73] Mayerberger, E.A., Street, R.M., McDaniel, R.M., Barsoum, M.W., Schauer, C.L., 2018. RSC Adv. 8, 35386–35394.
[74] Mayerberger, E.A., Urbanek, O., McDaniel, R.M., Street, R.M., Barsoum, M.W., Schauer, C.L., 2017. Journal of Applied Polymer Science 134, 45295.
[75] Mekuye, B., Abera, B., 2023. Nano Select 4, 486–501.
[76] Munshi, M.H., Hussain, S.A., Akter, M., Hakim, M.A., Hasan, M.A., Kabir, M.J., Kamruzzaman, M., Islam, T., 2026. ChemistrySelect 11.
[77] Nadaf, A., Gupta, A., Hasan, N., Fauziya, Ahmad, S., Kesharwani, P., Ahmad, F.J., 2022. RSC Adv. 12, 23808–23828.
[78] Nouseen, S., Pumera, M., 2025. Journal of Materials Chemistry A 34055–34084.
[79] Pan, S., Liu, L., Zhang, K., Wen, D., Wang, J., Qian, C., Xiao, X., He, Y., Ji, Z., Ying, G., 2026. Journal of Materials Science 61, 8418–8458.
[80] Panditkar, S.S., Gurnule, W.B., Waghe, P.U., Gurnule, P.W., Kumar, P., 2025. Polymer Bulletin 83, 53.
[81] Pang, Y., Li, J., Lv, K., Tang, D., Li, Q., 2024. New J. Chem. 48, 12477–12495.
[82] Pant, B., Park, M., Kim, A.A., 2023a. Micromachines 14, 1–19.
[83] Pant, B., Park, M., Kim, A.A., 2023b. Micromachines 14, 1–19.
[84] Parajuli, D., Murali, N., K. C, D., Karki, B., Samatha, K., Kim, A.A., Park, M., Pant, B., 2022. Polymers 14.
[85] Patial, S.K., Sharma, A., Singh, S., 2025. Synthesis and Fabrication Techniques of MXene, in: Moharana, S., Mahaling, R.N. (Eds.), Surface Engineering of MXenes. Springer Nature Singapore, Singapore, pp. 37–72.
[86] Peng, C., Wei, P., Chen, X., Zhang, Y., Zhu, F., Cao, Y., Wang, H., Yu, H., Peng, F., 2018. Ceramics International 44, 18886–18893.
[87] Pogorielov, M., Smyrnova, K., Kyrylenko, S., Gogotsi, O., Zahorodna, V., Pogrebnjak, A., 2021. Nanomaterials 11.
[88] Qian, M., Yan, X., Chen, Y., Guo, X.J., Lang, W.Z., 2022. Journal of Colloid and Interface Science 622, 11–20.
[89] Qin, X., Feng, X., Zhu, T., Ji, L., Zhu, A., 2022. Journal of Solid State Chemistry 312, 123142.
[90] Qu, F., Li, W., Dong, W., Tam, V.W.Y., Yu, T., 2021. Journal of Building Engineering 35, 102074.
[91] Rajasulochana, P., Preethy, V., 2016. Resource-Efficient Technologies 2, 175–184.
[92] Rasool, K., Mahmoud, K.A., Johnson, D.J., Helal, M., Berdiyorov, G.R., Gogotsi, Y., 2017. Scientific Reports 7, 1598.
[93] Raut, S., Sahoo, J.K., Sahoo, S.K., 2025. Journal of Molecular Liquids 433, 127871.
[94] Renkler, N.Z., Babar, Z.U.D., Barra, M., Cruz-Maya, I., De Santis, R., Girolamo, R. di, Marelli, M., Ferretti, A.M., Zaheer, A., Iannotti, V., Guarino, V., 2025. Macromolecular Materials and Engineering 310, 1–11.
[95] Riazi, H., Nemani, S.K., Grady, M.C., Anasori, B., Soroush, M., 2021. Journal of Materials Chemistry A 9, 8051–8098.
[96] Ruiz Rocha, J.E., Moreno Tovar, K.R., Navarro Mendoza, R., Gutiérrez Granados, S., Cavaliere, S., Giaume, D., Barboux, P., Jaime Ferrer, J.S., 2023. Nanomaterials 13.
[97] Said, Z., Sohail, M.A., Tabassum, H., Sajid, I.H., Ali, H.M., Jamil, F., Mishra, Y.K., Pandey, A.K., 2025. MXenes at the forefront: advances in energy storage and nanofluidic applications, Advanced Composites and Hybrid Materials. Springer International Publishing.
[98] SalehHudin, H.S., Mohamad, E.N., Mahadi, W.N.L., M. Afifi, A., 2021. Journal of Manufacturing Processes 62, 440–449.
[99] Santhamoorthy, M., Asaithambi, P., Perumal, I., Elangovan, N., Natarajan, P., Lin, M.-C., Kim, S.-C., Kumarasamy, K., Phan, T.T.V., 2025. Journal of Environmental Chemical Engineering 13, 117735.
[100] Seling, T.R., Songsart-power, M., Shringi, A.K., Paudyal, J., Yan, F., Limbu, T.B., 2025. 1–27.
[101] Shlapakova, L.E., Chernozem, R. V, Surmeneva, M.A., Liu, Y.-T., Zhang, S., Ding, B., Surmenev, R.A., 2026. Advanced Fiber Materials.
[102] Sun, A., Zhan, Y., Feng, Q., Yang, W., Dong, H., Liu, Y., Chen, X., Chen, Y., 2022. Journal of Membrane Science 663, 120933.
[103] Sun, Y., Lu, J., Li, S., Dai, C., Zou, D., Jing, W., 2024a. Separation and Purification Technology 331, 125640.

[104] Sun, Y., Lu, J., Li, S., Dai, C., Zou, D., Jing, W., 2024b. Separation and Purification Technology 331, 125640.
[105] Thakur, A., Kim, J., Wyatt, B.C., Gogotsi, Y., Anasori, B., 2026. Nature Reviews Materials.
[106] UNESCO World Water Assessment Programme (WWAP), Water for People, Water for Life: The United Nations World Water Devel_opment Report, 2003.
[107] Wang, A., Pan, R., Miao, J., Lin, Y., Deng, Y., Peng, S., Luo, X., Wu, P., Zhang, S., Wu, Y., Xie, J., Fan, T., 2025. 1–37.
[108] Wang, C., Park, M.J., Yu, H., Matsuyama, H., Drioli, E., Shon, H.K., 2022. Journal of Membrane Science 661, 120926.
[109] Wang, X., Shi, Y., Qiu, J., Wang, Z., 2023. Chem. Commun. 59, 5063–5066.
[110] Wang, Y., Pan, J., Zhang, Y., Ma, T., Zhao, J., Zhang, L., Yan, M., Zhang, S., 2024. Desalination 592, 118146.
[111] Wu, K., Galli, F., de Tommaso, J., Patience, G.S., van Ommen, J.R., 2025. Canadian Journal of Chemical Engineering 101, 1–13.
[112] Wu, S., Ma, S., Zhang, Q., Yang, C., 2025. Polymer 327, 128361.
[113] Wu, W., Li, X., Liu, Y., Liu, Z., Wang, Y., Jiao, T., 2025a. Progress in Organic Coatings 208, 109480.
[114] Wu, W., Li, X., Liu, Y., Liu, Z., Wang, Y., Jiao, T., 2025b. Progress in Organic Coatings 208, 109480.
[115] Xu, G., Mai, Z., Fu, W., Gonzales, R.R., Chiao, Y.H., Deng, L., Hu, M., Guan, K., Xu, P., Zhang, P., Li, Z., Matsuyama, H., 2024. Journal of Membrane Science 706, 122969.
[116] Xue, Q., Zhang, K., 2022. Membranes 12.
[117] Yan, M., Zhang, H., Deng, Y., Yang, T., Huang, J., Zhu, Y., 2023. Journal of Wuhan University of Technology-Mater. Sci. Ed. 38, 304–307.
[118] Yan, X., Yang, C., Ma, C., Tao, H., Cheng, S., Chen, L., Wang, G., Lin, X., Yao, C., 2022. Chemosphere 307, 136114.
[119] Yang, G.-Z., Li, H.-P., Yang, J.-H., Wan, J., Yu, D.-G., 2017. Nanoscale Research Letters 12, 55.
[120] Ye, S., Zhang, H., Lai, H., Xu, J., Yu, L., Ye, Z., Yang, L., 2024. Frontiers in Bioengineering and Biotechnology 12, 1–19.
[121] Yousefzadeh, M., Ramakrishna, S., 2017. 13 - Modeling performance of electrospun nanofibers and nanofibrous assemblies, in: Afshari, M. (Ed.), Electrospun Nanofibers, Woodhead Publishing Series in Textiles. Woodhead Publishing, pp. 303–337.
[122] Yu, H., Tan, Z., 2025. Electrospinning Parameters, in: Introduction to Electrospinning and Nanofiber. Springer Nature Switzerland, Cham, pp. 63–85.
[123] Zeng, G., Liu, Y., Lin, Q., Pu, S., Zheng, S., Ang, M.B.M.Y., Chiao, Y.H., 2022. Separation and Purification Technology 293, 121052.
[124] Zhang, C., Ma, Y., Zhang, X., Abdolhosseinzadeh, S., Sheng, H., Lan, W., Pakdel, A., Heier, J., Nüesch, F., 2020. Energy and Environmental Materials 3, 29–55.
[125] Zhang, D., Davoodi, P., Li, X., Liu, Y., Wang, W., Huang, Y.Y.S., 2020. Scientific Reports 10, 18783.
[126] Zhang, L., Liu, Y., Zeng, G., Yang, Z., Lin, Q., Wang, Y., Wang, X., Pu, S., 2023. Separation and Purification Technology 306, 122677.
[127] Zhou, J., Du, X., Lu, K., Xiao, A., 2025. Separation and Purification Technology 354, 129045.
[128] Zhou, L., Li, J., Xing, C., 2025. Chemical Engineering Journal 506, 159868.
[129] Zhu, M., Lu, C., Liu, L., 2023. iScience 26, 106718.
[130] Zhu, X., Zhang, N., Yuan, S., Zhang, J., Xu, H., Jiang, Z., Wang, Z., 2025. Journal of Membrane Science 734, 124495.
[131] Zhu, Y., Zhao, X., Guo, X., Greenfield, D.T., Duan, J., Lin, S., Hou, B., 2026. Progress in Organic Coatings 214, 110030.